

Quantum Sevalrty: Speed-up and Suppress Effect in Searching Problem

Jin-Hui Zhu,¹ Li-Hua Lu,¹ and You-Quan Li^{1,2,*}

¹Zhejiang Province Key Laboratory of Quantum Technology & Device and
Department of Physics, Zhejiang University, Hangzhou 310027, P.R. China.

²Collaborative Innovation Center of Advanced Microstructure, Nanjing University, Nanjing 210008, R.R. China.
(Received September 17, 2019)

The idea that a search efficiency can be increased with the help of a number of autonomous agents is often relevant in many situations, which is known among biologists and roboticists as a stigmergy. This is due to the fact that, in any probability-based search problem, adding information provides values for conditional probabilities. We report new findings of a speed-up and suppression effects occurring in the quantum search problem through the study of quantum walk on a graph with floating vertices. This effect is a completely counterintuitive phenomenon in comparison to the classical counterpart and may facilitate new insight in the future information search mechanisms that were never been perceived in classical picture. In order to understand the first passage probability, we also propose a method via ancillary model to bridge the measurement of the time dependence of the total probability of the complimentary part and the first passage probability of the original model. This is expected to provide new ideas for quantum simulation by means of qubit chips.

Searching and foraging has long been crucial topics in the ecology and microbiology [1, 2], it becomes enormously important in physics as well as in information science nowadays [3]. The idea that a search efficiency can be increased with the help of a number of autonomous agents was often relevant in many situations. Swarm communication is widely adopted among animals [4] and insects [5], and it is known among biologists [6] and roboticists [7] as a stigmergy. For example, in the search strategies of some predatory animals, which mix essentials of random-walk model with concentration on seasonal hot spots to find preys [8]. Similarly, in biological cells, peptide binding to transmembrane receptors relies on hydrophobic attraction superimposed on random Brownian motion [9]. Lévy walks are characterized by trajectories that have straight stretches for extended lengths whose variance is infinite [10]. Comparing to classical random walks, the Lévy walks were shown to being advantageous in optimality of search [11, 12]. Group Lévy foraging with an artificial pheromone communication between robots was studied [7] where the experimental results showed that if an interaction or exchange of information between the searchers is allowed the averaged search time can be decreased substantially. All those situations will continue to provide various questions for theorists [13].

Recently, modelling protein folding as a quantum walk on definite graphs reveals a fast protein-folding time [14]. This motivate us raise a general question whether quantum walk strategy can provide us any new insight on the searching efficiency [15]. Here we show our new findings that there are speed-up and suppression effects occurring in the quantum search problem that does not occur in its classical counterpart. We introduce a bilayer graph in which a layer of switchable vertices is floating over a main chain of vertices. We study the cases of the main chain only and compare successively with the case of one- and two-vertex on side chain connecting to the main chain. The mean first passage time starting from one terminal to the other terminal are calculated and the effect caused by connecting one or two vertices from the side-chain

are investigated. As the search efficiency can be quantitatively measured by the mean first passage time [16, 17], we investigate various situations of our model in the framework of the classical random walk and quantum walk, respectively. We also introduce reduced density matrix and calculate the von Neumann entropy to get certain knowledge about the counterintuitive effect. In order to understand the first passage probability, we also propose a method via ancillary model to bridge the measurement of the time dependence of the total probability of the complimentary part and the first passage probability of the original model. Quantum search's feature is due to its parallel calculation strategy and quantum coherence nature. It is expected to provide new ideas for quantum simulation by means of qubit chips.

Model system and the mean first passage time: We consider a two layer system that consists of a back layer (base layer) of a chain of N vertices and a front layer (float layer) of several initially isolated vertices which are switchable to connect with the contact-vertex in base layer. In the float layer, another neighbor vertex can also be switched on or off from the aforementioned connected vertex in the float layer (Fig. 1). Thus, we investigate a model of a main chain of N vertices

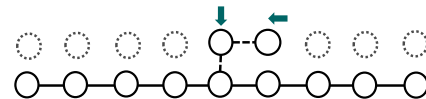


FIG. 1. **Graphical illustration of the model Hamiltonian.** Here the dash-line circle denotes isolated vertex in the float layer that can be pushed to connect with a vertex in the base layer. If another neighbor in the float layer is sheared to connect with, a side chain of two vertices is tuned on then.

along with a side chain of S vertices mounted at the center. In the model, the number of the side chain can be changed by tuning up one more vertex, that means the S can be changed from odd number to even number, or vise versa. We explore how does the side chain affect the mean first passage time that

costs from initial site, saying vertex-1, to target site, saying vertex- N . The mean first passage time is defined as an integrand, namely,

$$\tau = \int_0^{\tau_0} t F_{1,N}(t) dt / \int_0^{\tau_0} F_{1,N}(t) dt, \quad (1)$$

where $\tau_0 = \infty$ in the classical random walk while it ought to be determined by $F_{1,N}(\tau_0) = 0$ in quantum-walk problem [14]. Here $F_{1,N}(t)$ is determined by the convolution relation [18–22],

$$P_{1,N}(t) = \int_0^t F_{1,N}(t') P_{N,N}(t-t') dt', \quad (2)$$

where $P_{a,b}(t)$ is the time-dependent probability distribution at vertex- b evolving from a initial distribution located merely at vertex- a , i.e., $P_{a,b}(0) = \delta_{ab}$.

The classical random walk: Random walks on a graph (Fig. 1) is described by the probability distribution over the vertices, namely, $p_a(t)$ with $a = 1, 2, \dots, N, N+1, N+2, \dots, N+S$ obeying the following master equation,

$$\frac{d}{dt} p_a(t) = \sum_b K_{ab} p_b(t). \quad (3)$$

Here $K_{ab} = J_{ab}/\text{deg}(b) - \delta_{ab}$ with J_{ab} being the adjacency matrix of the graph and $\text{deg}(b) = \sum_c J_{cb}$ the degree of vertex- b . Let us first observe the classical random walk on the graph (Fig. 1) for $S = 0, 1$ and 2 one by one. For each case, we solve the master equation (3), respectively, under the initial condition $p_1(0) = 1$ and another initial condition $p_N(0) = 1$. Those solutions provide us $P_{1,a}(t)$ and $P_{N,a}$ that determine the so-called first passage probabilities [18–22] $F_{1,N}(t)$ through the convolution relation (2). Strictly speaking, the $F_{a,b}(t)$ measures a probability per unit time. After solving the time dependence $F_{1,N}(t)$, we can evaluate the mean first passage time as an integrand defined by Eq. (1).

We numerically solve the random walk on systems with different number of vertices on the main chain, saying $N = 3, N = 5, \dots$, till $N = 43$. The solution of $N = 9$ is plotted in Fig. S1 and the relevant quantities for solving the first passage probabilities are plotted in Fig. 2. We calculate the mean first passage time from vertex-1 to vertex- N , and denote the obtained value for $S = 0$ by τ_c , that for $S = 1$ by τ'_c and that for $S = 2$ by τ''_c . Here the subscript ‘‘c’’ refers the magnitude from classical random walk. Our results exhibit that τ'_c is always larger than τ_c and τ''_c is always larger than τ'_c (Fig. 2C and Table S1). This manifests that an additional vertex connected from the float layer always retards the mean first passage time [19] of classical random walk in some sense, which just fits with the daily conventional intuition.

Quantum severalty: The quantum walk [23–25] on a graph is described by the time-dependent wavefunction $|\Psi(t)\rangle = \sum_{a=1}^{N+S} \psi_a(t) |a\rangle$ that obeys the Schrödinger equation,

$$i\hbar \frac{d}{dt} |\Psi(t)\rangle = \hat{H} |\Psi(t)\rangle. \quad (4)$$

Here the Hamiltonian $\hat{H} = \sum_{ab} J_{ab} |a\rangle\langle b|$ is defined by the adjacency matrix J_{ab} of the graph. After solving Eq. (4) under the initial condition $|\Psi(0)\rangle = |1\rangle$ and another initial condition $|\Psi(0)\rangle = |N\rangle$, respectively, we get $P_{1,N}(t) = |\psi_N^{(1)}(t)|^2$ and $P_{N,N}(t) = |\psi_N^{(N)}(t)|^2$ (the superscript is introduced to distinguish solutions from different initial conditions), then obtain $F_{1,N}(t)$ from the convolution relation (2). We solve the quantum mechanical problem for the cases $S = 0, 1$ and 2 one by one and furthermore evaluate the mean first passage time in terms of the solved $F_{1,N}(t)$. The time dependence of $P_{1,N}(t)$, $P_{N,N}(t)$ and $F_{1,N}(t)$ in quantum case for $N = 9$ are plotted in Fig. 2D-2F.

The calculated mean first passage time is given in the inserted panel of Fig. 2F. We can see $\Delta_1 = \tau' - \tau < 0$, which implies that the mean first passage time for $S = 1$ is shorter than that for $S = 0$. Unlike the classical case where an additional vertex at side chain will increase the mean first passage time (retard the searching rapidity), quantum mechanically, it will speed up the searching rapidity (decrease the mean first passage time). Our result from the quantum walk reveals a novel effect that is a completely counterintuitive phenomenon. In comparison to its classical counterpart, we suggest to call it ‘‘quantum severalty’’. This is true not only for $N = 9$, but also for other number of vertices. We also calculate $N = 3, 5, \dots$, till 43 (Table S1) and plot the speed-up ratio Δ_1/τ as a function of N , the number of the vertices on the main chain (Fig. 2G). The fitted curve fulfills a power law behavior (see the inserted panel of Fig. 2G), namely,

$$\frac{\Delta_1}{\tau} \approx -0.4574N^{-0.714}.$$

If connecting one more vertex to the already connected one on the side chain, we find that $\Delta_2 = \tau'' - \tau$ turns to be a tiny magnitude. This means tuning on a second vertex on the side chain, the original speed up effect will be suppressed down at once. The suppression magnitude $\Delta'_2 = \tau'' - \tau' = \Delta_2 - \Delta_1 > 0$. The relative suppression ratio Δ_2/τ versus the site number N is shown in Fig. 2H. Thus, if one float vertex is pushed to connect with the base layer, we attain a significant speed up effect; furthermore, if a second nearby float vertex is sheered to connect with the connected float vertex, it causes a suppression effect. It is also worthwhile to know what happens if the side chain is not mounted at the center of the main chain. Denoting the central position as c , we discuss the case when the side chain is on the position $c \pm 1, c \pm 2$ etc.. Our calculation results exhibit that the speed-up and suppress effect still exists if the the side chain is mounted nearby the center, and the magnitude changes are just affected slightly (Table S2).

To help an understanding about the aforementioned quantum severalty, we consider a reduced 2 by 2 density matrix $\tilde{\rho}$ in the spirit of Ref. [26] that may maintain certain information of quantum coherence. Because the graph characterising our model system is actually a two-color graph (i.e., minimally, two colors are needed to dye every vertices without the occurrence of neighbor vertices sharing the same color), we are able to define the 2 by 2 density matrix $\tilde{\rho}$ in

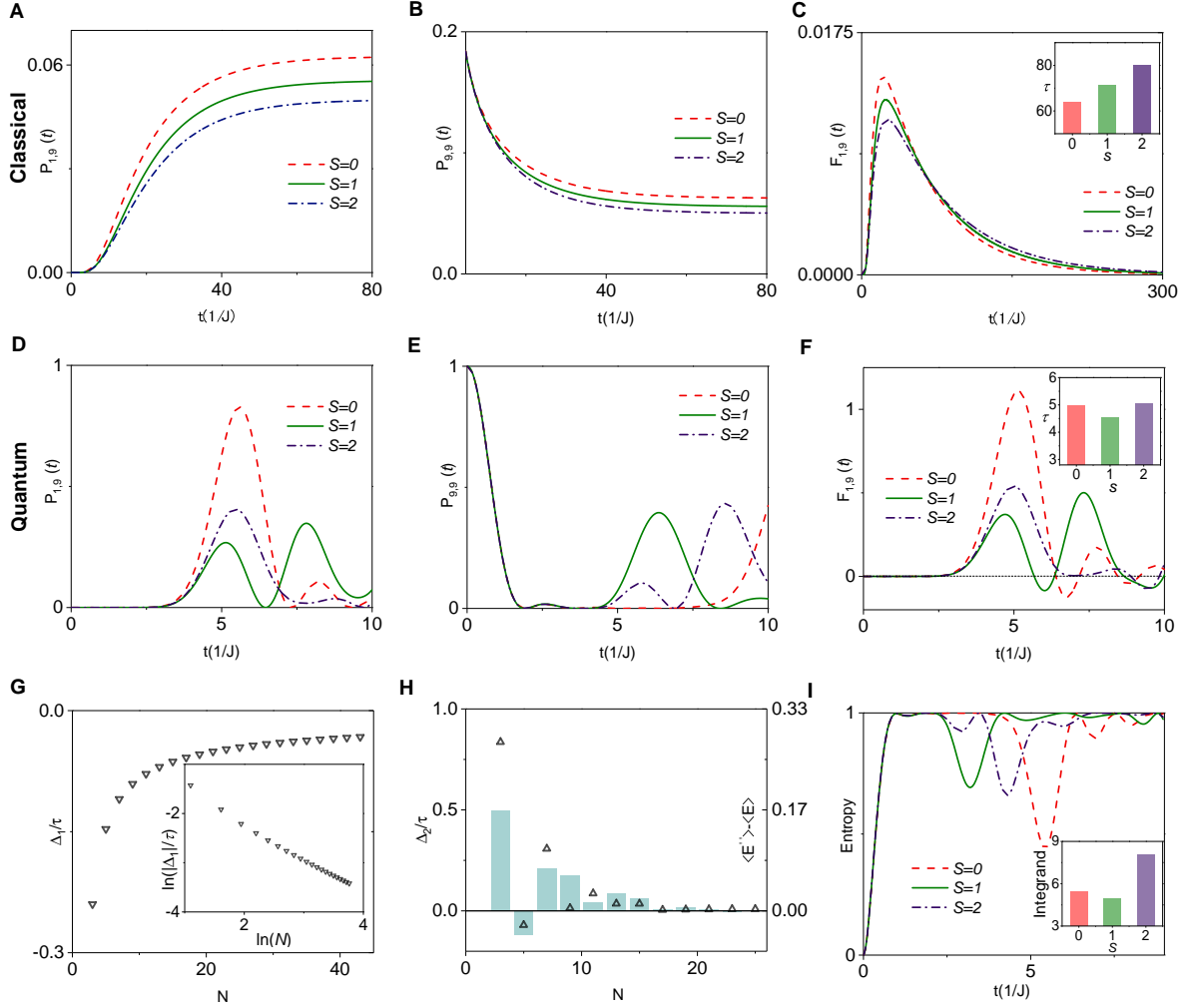


FIG. 2. **Classical and quantum solutions, their features of the mean first passage time:** The time dependence of (A) $P_{1,9}(t)$, (B) $P_{9,9}(t)$ and (C) $F_{1,9}(t)$ solved from classical random walk; the time dependence of (D) $P_{1,9}(t)$, (E) $P_{9,9}(t)$ and (F) $F_{1,9}(t)$ solved from quantum walk for $N = 9$. (G) The quantum speed-up ratio Δ_1/τ versus the number of sites N , the inserted panel is the logarithm scaled plot indicating a power law behavior. (H) The relative suppression ratio Δ_2/τ versus the number of sites N , presented by small triangular, together with the magnitude difference between the averaged von Neumann entropies for $S = 2$ and $S = 0$ presented by histogram which is scaled by the right vertical axis. (I) The time dependence of von Neumann entropies for $S = 0, 1, 2$ when $N = 9$. Their integrands are shown in the inserted panel.

terms of $\tilde{\rho}_{11} = \sum_{a_1} \psi_{a_1} \psi_{a_1}^*$, $\tilde{\rho}_{22} = \sum_{a_2} \psi_{a_2} \psi_{a_2}^*$, $\tilde{\rho}_{12} = \sum_{a_1 a_2} \psi_{a_1} \psi_{a_2}^* / \sqrt{n_1 n_2}$ and $\tilde{\rho}_{21} = \tilde{\rho}_{12}^*$ where n_1 and n_2 stand for, respectively, the total numbers of the vertices in the same color and the square-root-denominator factor in the summation guarantees the reduced density matrix such as defined is of non-negatively definite. Then the von Neumann entropy [27] is given by $E(\tilde{\rho}) = -\text{tr}(\tilde{\rho} \log_2 \tilde{\rho})$ whose time dependence for $N = 9$ is plotted in Fig. 2I. We denote the von Neumann entropies for $S = 0, 1, 2$ respectively by E , E' and E'' , of which the integrand over the whole period τ_0 is indicated by histograms in the inserted panel. One can also make an average of the von Neumann entropy, $\langle E \rangle = \int_0^{\tau_0} E(t) dt / \tau_0$, clearly, the difference $\langle E'' \rangle - \langle E \rangle$ have something to do with the Δ_2/τ - N dependence (Fig. 2H). All these features are true also for $N = 3, 5, \dots$ (Fig. S2).

Implications of the first passage probability: Classically, the first passage probability $F(t)$ can be obtained directly via ensemble simulation. A numerical simulation of one million ensembles gives rise to a first-passage probability that fit well with the convolution results (Fig. S3). We know that the one dimensional random walk can be demonstrated by billiards scattered by periodically placed nails (Fig. 3A). In order to understand the physics implication of the first passage probability $F_{1,N}(t)$, we make some changes on the set-up frequently adopted in science and technology museum. Pouring in billiards from the hole close to the left edge, keeping the right-side boundary open and placing an array of collectors to receive, successively, the billiard scattered toward outside, we will have a $F_{1,N}(t)$ after sufficient billiards were poured in. The magnitudes of $F_{1,N}(t)$ is valued by accounting the bil-

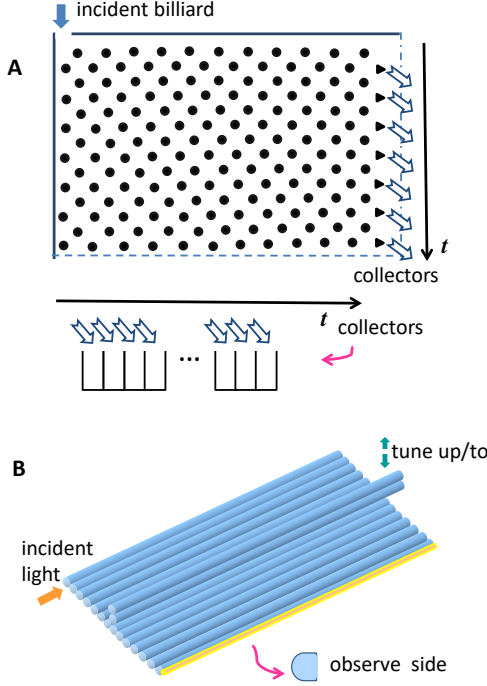


FIG. 3. **Proposals for experiment set-up:** (A) Demonstration experiment set-up for random walk. This set-up is mounted vertically so that the gravitational force naturally provide us the time order direction. The collectors on the right-side are labelled by this time order. (B) Experiment scheme for quantum walk via optical fibre. Incident beam of light is applied from one side and the observation is made on the other side of which the lateral fibre is cut to form a unreflecting surface. The speed up effect, and furthermore a suppress effect will be observed by tuning up or tuning to the additional fibre.

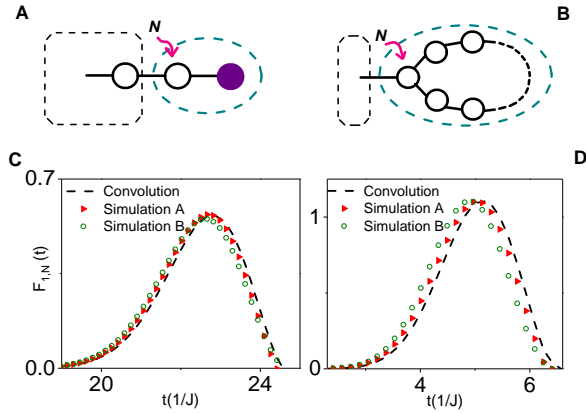


FIG. 4. **Quantum simulation scheme via qubit chip:** (A) Ancillary model with a sticky tail, which is obtained by connecting to the N -th vertex with an additional sticky vertex; (B) Ancillary model dressed with a ring, which is a prolongation of the N -th vertex to be a ring of several more vertices; (C) The first passage probability obtained, respectively, by means of the above proposals for $N = 43$, and (D) that for $N = 9$. The datas obtained via convolution relation are also plotted to compare.

simulation (Fig. S3) on classical random walk can be realized by such a demonstration experiment (Fig. 3A).

The aforementioned classical set-up motivated us, at once, to propose a quantum simulation experimental scheme. One can make a set-up (Fig. 3B) in terms of optical fibre [28] by cutting a lateral fibre to form a reflectionless surface, then the observed intensity along the fibre will be the $F_{1,N}(t)$. One can also observe the new phenomena we found previously [29], i.e., the speed up and suppress effects caused by tuning up or tuning down side-chain optical fibre.

Quantum simulation by qubit chips: We propose possible experiment design (Fig. 4) to carry out quantum simulations [30] via qubit chips. To measure the first passage probability $F_{1,N}(t)$ at vertex- N , we can either connect an additional sticky vertex to that vertex (Fig. 4A) or make a prolongation of that vertex to be a ring of several more vertices (Fig. 4B). For the former proposal (Fig. 4A), as we know, in the presence of sticky, we need to solve the density matrix from the Lindblad equation [31]

$$\frac{d}{dt}\tilde{\rho} = \frac{1}{i\hbar}[\tilde{H}, \tilde{\rho}] + \frac{\lambda}{2}(2L\tilde{\rho}L^\dagger - \tilde{\rho}L^\dagger L - L^\dagger L\tilde{\rho}), \quad (5)$$

where $\tilde{H} = \hat{H} + V |N+1\rangle\langle N+1|$ with V being the negative potential on the sticky vertex, and $L = |N\rangle\langle N+1|$ the Lindblad operator. Once the density matrix $\tilde{\rho}_{ab}(t)$ ($a, b = 1, 2, \dots, N, N+1$) is solved for the ancillary model with a sticky tail (Fig. 4A), we are able to obtain the first passage probability:

$$F_{1,N}(t) = -\frac{1}{A} \frac{d}{dt} \sigma(t), \quad (6)$$

where $\sigma(t) = \sum_{a=1}^{N-1} \tilde{\rho}_{aa}(t)$ and A is a normalization constant so that $\int_0^{\tau_0} F_{1,N}(t) dt = 1$, i.e., $A = \sigma(\tau_0)$. If the realization of the sticky vertex in some experimental system is uneasy, an alternative proposal is to prolong the vertex N to be a ring of several qubits (Fig. 4B), we call it the ancillary model dressed with a vertices ring. With this ancillary model, one is still able to simulate the $F_{1,N}(t)$ by the same formula (6), but, with the $\sigma(t)$ given by $\sigma(t) = \sum_{a=1}^{N-1} |\tilde{\psi}_a^{(1)}(t)|^2(t)$. Our quantum simulation results for $N = 43$ together with the convolution result are plotted in Fig. 4C, where the parameter choices are $\lambda = 4.6$, $V = -2.3J$ and the ring of 44 vertices. Fig. 4D shows that for $N = 9$ with parameter choices $\lambda = 5$, $V = -2.5J$ and the ring of 10 vertices. Therefore, there is a bridge between the probability measurement of the ancillary model and the first passage probability of the original model, which will shed new light on the research area of quantum simulation.

This work is supported by National Key R & D Program of China, Grant No. 2017YFA0304304 and NSFC, Grant No. 11935012.

liards received by those collectors labelled by the t . Thus, our

* email: yqli@zju.edu.cn

- [1] M. F. Shlesinger, Mathematical physics: Search research. *Nature* **443**, 281-282 (2006).
- [2] O. Bénichou, C. Loverdo, M. Moreau, & R. Voituriez, Two-dimensional intermittent search processes: An alternative to Lévy flight strategies. *Phys. Rev. E* **74**, 020102 (2006).
- [3] I. Foulger, S. Gnutzmann, & G. Tanner, Quantum search on graphene lattices. *Phys. Rev. Lett.* **112**, 070504 (2014).
- [4] W. J. Bell, *Searching Behavior* (Springer Science plus Business Media Dordrecht 1990)
- [5] V. G. Dethier, Communication by insects: physiology of dancing. *Science* **125** 331 (1957).
- [6] G. Ariel, A. Rabani, S. Benisty, J. D. Partridge, R. M. Harshey, & A. Béer, Swarming bacteria migrate by Lévy Walk. *Nat. Commun.* **6**, 8396 (2015)
- [7] R. Fujisawa & S. Dobata, Lévy walk enhances efficiency of group foraging in pheromone-communicating swarm robots. *Proceedings of the 2013 IEEE/SICE International Symposium on System Integration, Kobe, Japan* (IEEE, New York 2013) pp. 808C813.
- [8] O. Bénichou & S. Redner, Depletion-controlled starvation of a diffusing forager. *Phys. Rev. Lett.* **113**, 238101 (2014).
- [9] J. Kennedy & R. Eberhart, *Swarm Intelligence* (Morgan Kaufmann, Burlington, MA 2001).
- [10] J. Klafter, M. F. Shlesinger, & G. Zumofen, Beyond Brownian motion. *Physics Today* **49**, 2, 33 (1996).
- [11] M. Shlesinger, J. Klafter, & B. J. West, Lévy walks with application to turbulence and chaos. *Physica* (Amsterdam) **140A**, 212 (1986).
- [12] G. M. Viswanathan, S. V. Buldyrev, S. Havlin, M. G. E. da Luz, E. P. Raposo, & H. E. Stanley, Optimizing the success of random searches. *Nature* **401**, 911 (1999).
- [13] V. Zaburdaev, S. Denisov, & J. Klafter, Lévy walks. *Rev. Mod. Phys.* **87**, 483 (2015).
- [14] L. H. Lu & Y. Q. Li, Quantum approach to fast protein-folding time. *Chin. Phys. Lett.* **36**, 080305 (2019).
- [15] H. Tang, C. D. Franco, Z. Y. Shi, T. S. He, Z. Feng, J. Gao, K. Sun, Z. M. Li, Z. Q. Jiao, T. Y. Wang, M. S. Kim, & X. M. Jin, Experimental quantum fast hitting on hexagonal graphs. *Nat. Photon.* **12**, 754 (2018).
- [16] H. Friedman, D. A. Kessler, & E. Barkai, Quantum walks: The first detected passage time problem. *Phys. Rev. E* **95**, 032141 (2017).
- [17] J. G. Muga & C. R. Leavens, Arrival time in quantum mechanics. *Physics Reports* **338**, 353 (2000).
- [18] E. W. Montroll, Random walks on lattices III: calculation of first-passage times with application to exciton trapping on photosynthetic units. *J. Math. Phys.* **10**, 753 (1969).
- [19] S. Redner, *A guide to first-passage processes* (Cambridge Univ. Press, Cambridge, 2001).
- [20] J. D. Noh & H. Rieger, Random walk on complex networks. *Phys. Rev. Lett.* **92**, 118701 (2004).
- [21] S. Condamin, O. Bénichou, V. Tejedor, R. Voituriez, & J. Klafter, First-passage times in complex scale-invariant media. *Nature* **450**, 77 (2007).
- [22] T. Guérin, N. Levernier, O. Bénichou, & R. Voituriez, Mean first-passage times of non-Markovian random walkers in confinement. *Nature* **534**, 356 (2016).
- [23] Y. Aharonov, L. Davidovich, & N. Zagury, Quantum random walks. *Phys. Rev. A* **48**, 1687 (1993).
- [24] E. Farhi & S. Gutmann, Quantum computation and decision trees. *Phys. Rev. A* **58**, 915 (1998).
- [25] K. Manouchehri & J. B. Wang, *Physical implementation of quantum walks* (Springer-Verlag, Berlin, 2014).
- [26] W. W. Mao, L. H. Lu, Y. Y. Ji, & Y. Q. Li, Quantum intelligence on protein-folding pathways. arXiv:1907.07179
- [27] M. A. Nielsen & I. L. Chuang, *Quantum computation and quantum information* (Cambridge Univ. Press, Cambridge, 2000).
- [28] H. B. Perets, Y. Lahini, F. Pozzi, M. Sorel, R. Morandotti, & Y. Silberberg, Realization of quantum walks with negligible decoherence in waveguide lattices. *Phys. Rev. Lett.* **100**, 170506 (2008).
- [29] Even more, if the optical fibres are sufficient long, there may exist a 'dark period' which we mean the time interval that the solved first passage probability becomes negative.
- [30] I. M. Georgescu, S. Ashhab, & F. Nori, Quantum simulation. *Rev. Mod. Phys.* **86** 153 (2014).
- [31] G. Lindblad, Generators of quantum dynamical semigroups. *Commun. Math.* **48**, 119 (1976).